16 November 2001

Chemical Physics Letters 348 (2001) 491–496

CHEMICAL PHYSICS LETTERS

www.elsevier.com/locate/cplett

A new intermolecular potential for liquid oxygen

Baw-Ching Perng [a], Shogo Sasaki [a], Branka M. Ladanyi [a,1], K.F. Everitt [b], J.L. Skinner [b,*]

[a] *Department of Chemistry, Colorado State University, Fort Collins, CO 80523, USA*
[b] *Department of Chemistry, Theoretical Chemistry Institute, University of Wisconsin, 1101 University Avenue, Madison, WI 53706, USA*

Received 25 July 2001; in final form 20 September 2001

Abstract

We develop a new two-site Lennard-Jones intermolecular potential model for liquid oxygen where the two sites are centered on the nuclear positions. The Lennard-Jones ϵ and σ parameters are determined by fitting experimental thermodynamic data in the liquid region of the phase diagram to results from molecular dynamics simulations. This procedure yields $\epsilon/k = 48$ K, and $\sigma = 3.006$ Å. Using this potential we then calculate, again from molecular dynamics simulations, the static structure factor (or site–site radial distribution function) and the second-rank rotational time-correlation function. In both cases our results are in excellent agreement with experiment (from X-ray scattering and depolarized Raman spectroscopy, respectively). © 2001 Published by Elsevier Science B.V.

1. Introduction

Accurate intermolecular potentials are essential for quantitatively describing the structure and dynamics of condensed-phase systems. In this Letter we focus on liquid oxygen, the reasons for which are threefold. First, oxygen is a homonuclear diatomic, and so its theoretical description is relatively straightforward (although it is an electronic triplet). Second, there are numerous thermodynamic, spectroscopic and scattering experiments on liquid oxygen, which provide important benchmarks for any theoretical model. And third, we are interested in understanding vibrational energy relaxation in liquid oxygen [1–3], and for a theoretical description of this process it is very important to have an accurate intermolecular potential. The goal of this Letter is to develop a simple intermolecular potential that is consistent with a variety of different experiments.

Several model potentials for O_2 are available in the literature [4–10]. Of these, the two site Lennard-Jones (2LJ) model is perhaps the most appealing, due to its simplicity. In this model the intermolecular interaction occurs through two sites on each molecule, and the site–site potential takes the Lennard-Jones form. Specification of the Lennard-Jones parameters ϵ and σ, and the intramolecular site–site distance l, then determines the model for the intermolecular potential energy. The

* Corresponding author. Fax: +1-608-262-9918.
E-mail addresses: bl@bibm.mfbl.colostate.edu (B.M. Ladanyi), skinner@chem.wisc.edu (J.L. Skinner).
[1] Fax: +1-970-491-3361.

0009-2614/01/$ - see front matter
PII: S0009-2614(01)01152-6

2LJ model has been used to describe several properties of liquid oxygen, including the gas–liquid coexistence curve [4,11,12], neutron scattering [13], and Raman and Rayleigh spectroscopy [7,9,14–17]. In many cases the agreement between theory and experiment is reasonable, although different parameter sets were used for the various calculations. We note in passing that for N_2 a single 2LJ potential does satisfactorily describe all these properties [18].

At least in terms of thermodynamics, the most promising of the various 2LJ potentials is due to Bohn et al. [4], who used perturbation theory to fit the parameters ϵ, σ, and l to thermodynamic data for the liquid–gas coexistence curve. It was subsequently demonstrated by molecular dynamics simulation [11] that the predicted thermodynamic properties are in excellent agreement with the experimental data [19] for oxygen over a large range of the fluid phase diagram. In this potential, which we call the BLF potential, $l = 0.7063$ Å, which is quite a bit shorter than the experimental bond length (the distance between the nuclei) of $r_e = 1.208$ Å. Now there is no fundamental reason why the interaction sites should be centered on the nuclei. Nonetheless, this difference between the intersite distance and the bond length is much larger than for similarly optimized potentials for other homonuclear diatomics [4], and is possibly related to the fact that oxygen is a triplet.

In fact, whereas the thermodynamic predictions of a particular 2LJ model are quite dependent on the intersite distance, they are independent of the positions of the nuclei (since the molecules only interact through the sites). However, certain microscopic structural and dynamic properties will depend on the positions of the nuclei, and so to describe these microscopic properties with a 2LJ model one must specify the nuclear positions. For example, for the BLF potential there are an infinite number of choices, but only two simple ones: put the nuclei on the sites, or farther apart so that the molecule has the correct experimental bond length. We will call these two models the 'short BLF' and 'long BLF' model, respectively. The first model has the clear drawback that the moment of inertia of the molecule is too small, and so at least the rotational dynamics are not correct, while the second model has the correct moment of inertia but is still somewhat unsettling and unintuitive since the sites are so far inside the molecule.

For the BLF model at 77 K we have calculated the site–site radial distribution function $g(r)$ using molecular dynamics simulation, and its Fourier transform $\hat{S}(k)$. These results are independent of the nuclear positions. Since X-rays scatter off electrons, and the sites in the 2LJ model are the centers of the molecules' electron distribution, it is appropriate to compare our simulation results for $g(r)$ and $\hat{S}(k)$ to experimental results from X-ray scattering [20–22]. We find substantial disagreement between the two (see below). We have also calculated the second-rank rotational time-correlation function $\phi_2(t)$ for both the short and long BLF models at 77 K. $\phi_2(t)$ has been determined experimentally from depolarized Raman experiments [23]. For each of the two models, simulation and experiment are again not in good agreement. This motivated us to develop a new 2LJ potential that adequately describes thermodynamic as well as structure and dynamics experiments. To this end we decided to restrict ourselves to the class of models where the intersite distance is equal to the experimental bond length.

The development of this new potential and comparison of its thermodynamics with experiment is discussed in Section 2. In Section 3, for the BLF models and the new model we calculate $g(r)$, $\hat{S}(k)$, and $\phi_2(t)$, and compare with experiment. We find that results for the new potential are in excellent agreement with both experiments.

2. New intermolecular potential for liquid oxygen

To develop the potential, as mentioned above we set $l = r_e = 1.208$ Å, and vary the parameters ϵ and σ over ranges that are reasonable for second row atoms. For each pair of ϵ and σ we calculate, using a molecular dynamics simulation, the excess internal energy, ΔU (which corresponds to the average intermolecular potential energy), and pressure, P, for a set of densities and temperatures in the liquid phase.

The simulation results were obtained within the microcanonical ensemble on systems of 256 rigid

Table 1
Comparison of experimental and simulation data for the thermodynamic properties of O_2 for the new 2LJ potential

T (K)	ρ (nm^{-3})	P (sim) (MPa)	P (expt) (MPa)	ΔU (sim) (kJ mol^{-1})	ΔU (expt) (kJ mol^{-1})
126	20.91	62.0 ± 1.2	56.4	-5.592 ± 0.004	−5.687
116	20.66	36.6 ± 1.0	32.4	-5.604 ± 0.004	−5.711
106	21.07	17.3 ± 1.0	18.3	-5.720 ± 0.003	−5.839
96	20.79	3.8 ± 0.9	3.5	-5.870 ± 0.003	−5.981
80	22.41	1.8 ± 1.3	0.1	-6.360 ± 0.003	−6.457
70	23.28	0.7 ± 0.9	0.1	-6.690 ± 0.004	−6.751

(non-vibrating) molecules. Time steps of 2.85 fs were used to integrate the equations of motion using the Verlet algorithm [24] for translation and the Singer algorithm for rotation [25]. The LJ interactions were truncated at half of the box length of the cubic simulation cell and the long-range corrections to P and ΔU were computed using the expressions given by Singer et al. [25]. The final results for each state point represent averages over about 50 000 time-step trajectories. These trajectory data were collected after an equilibration period of several thousand time steps for each state.

Considering data in the liquid state over the temperature range of 70–126 K and density range of 20.66–23.28 nm^{-3}, we find that the best-fit parameters are $\sigma = 3.006$ Å and $\epsilon/k = 48$ K. Table 1 shows that the agreement of the results obtained by molecular dynamics simulation for this potential and the experimental data [19] for P and ΔU is reasonably good, although not quite as good as for the BLF model [11] (as expected, since we have one fewer adjustable parameter).

Perhaps surprisingly, this 2LJ model also predicts the critical parameters for oxygen quite accurately. The reduced bond length, $l^* = l/\sigma$, uniquely determines the reduced critical temperature and density, $T_c^* = kT_c/\epsilon$ and $\rho_c^* = \rho_c\sigma^3$, of the 2LJ fluid. Kriebel et al. [12] determined these parameters for 2LJ fluids for a range of l^*. Linearly interpolating the values of ρ_c^* and $1/T_c^*$ listed in [12, Table 5] to the relevant value of $l^* = 0.402$ yields a prediction of the critical parameters, $T_c = 153.5$ K and $\rho_c = 8.43$ nm^{-3}, in good agreement with the accepted experimental values, $T_c = 154.6$ K and $\rho_c = 8.21$ nm^{-3}.

3. Structure and dynamics of liquid oxygen

In this section we compare theoretical predictions for structural and dynamical properties of liquid oxygen at 77 K and 1 atm pressure for each of three (short BLF, long BLF, and new) 2LJ models. The parameters for the three models are listed in Table 2.

The molecular dynamics simulations used to calculate these properties involved 500, or in some cases 2916, oxygen molecules in a cubic box with periodic boundary conditions. The density was $\rho = 22.64$ nm^{-3}, which is the experimentally [19] determined liquid density at a pressure of 1 atm and 77 K. The intermolecular potential was truncated at half the box length, and the Leapfrog algorithm [26] was used to integrate the equations of motion with a time-step of 4 fs. The liquid was initially equilibrated at 320 K for 50 000 time-

Table 2
2LJ parameters and calculated center-of-mass diffusion constant, D, for the three models of liquid oxygen

Model	ϵ/k (K)	σ (Å)	l (Å)	r_e (Å)	D (10^{-5} cm^2 s^{-1})
New	48.0	3.006	1.208	1.208	1.89
Short BLF	38.003	3.2104	0.7063	0.7063	1.34
Long BLF	38.003	3.2104	0.7063	1.208	1.29

steps, the temperature was periodically scaled to the final simulation temperature (77 K) over 50 000 time-steps, and the liquid was equilibrated at the final temperature for at least 50 000 time-steps. Using this procedure the final simulation temperature was reproducibly 77 ± 0.3 K.

3.1. Static structure

One way to describe the static structure of the fluid is with $g(r)$, the intermolecular radial distribution function for the site positions. $g(r)$ can be measured experimentally by X-ray scattering through the static structure factor, which for homonuclear diatomic molecules is defined to be [27]

$$\hat{S}(k) = \frac{1}{2N}\left\langle \sum_{ij} e^{i\vec{k}\cdot(\vec{r}_i - \vec{r}_j)} \right\rangle, \tag{1}$$

where $\vec{r}_i$ labels the position of the ith site, the summations are over all sites, and N is the number of sites (atoms) in the system. Using equilibrium statistical mechanics it can be shown that $\hat{S}(k)$ and $g(r)$ are related (for $k \neq 0$) by [27,28]

$$\hat{S}(k) = \frac{1}{2}\left[1 + \frac{\sin(kl)}{kl}\right] + \frac{4\pi\rho}{k}\int_0^\infty dr\, r[g(r) - 1]\sin(kr), \tag{2}$$

where ρ is the (molecular) number density.

For each model potential we obtain $g(r)$ from the simulation of 2916 molecules; the results (the short BLF and long BLF models give identical results for the site–site $g(r)$) are shown in Fig. 1. One sees significant differences between the BLF and new models. In particular, for the new model the first peak shows a shoulder, and the overall amplitude of the structure is smaller. Also shown in Fig. 1 are the experimental results from X-ray scattering [20] for liquid oxygen at 77 K and 1 atm pressure. Except for a small discrepancy at the first peak, the agreement between experiment and simulation for the new model is excellent.

It is also interesting to compare simulation and experiment for $\hat{S}(k)$ directly, since that is what is actually measured experimentally. This comparison in principle yields no additional information (beyond what is obtained from the $g(r)$ comparison), but does provide a consistency check of the theoretical and experimental inversion procedures. Our results for $g(r)$ are of course only meaningful out to half the box length. Even for the larger simulation size of 2916 molecules, near the cutoff $g(r)$ is still oscillating and has not yet become 1. If we are to describe $\hat{S}(k)$ at small k, we need to describe accurately the large r behavior of $g(r)$. To this end, we have fit [29] $g(r)$ for $r > 0.5$ nm to the form of

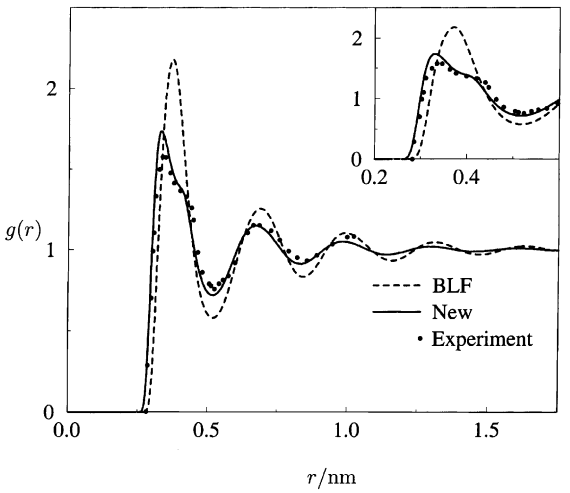

Fig. 1. Intermolecular radial distribution function for the site positions in liquid oxygen at 77 K and 1 atm pressure: simulation results for the BLF and new models, and experiment. The inset emphasizes the shape of the first peak.

$$g(r) = Ae^{-\alpha r^\beta}\cos(\gamma r + \phi) + 1. \tag{3}$$

We find that in both cases the fit is excellent, and the decay of the envelope is nearly exponential, as expected for fluids with short-ranged interactions [30]. We now use this form to extend our radial distribution functions out to arbitrarily large distances.

Using Eq. (2) and $g(r)$ from simulation (and its extrapolation) we compute $\hat{S}(k)$ for the BLF and new models, and the results are shown in Fig. 2. In this case the differences between the two models are even more accentuated. Also shown in Fig. 2 is the experimental $\hat{S}(k)$, as measured by Furomoto and Shaw [20], tabulated by Schmidt and Tompson [21], and plotted by Dore et al. [22]. The agreement between experiment and simulation for the new model is again excellent.

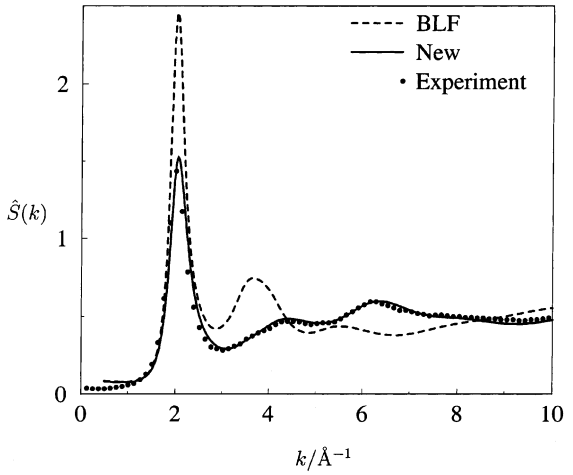

Fig. 2. X-ray structure factor for liquid oxygen at 77 K and 1 atm pressure: simulation results for the BLF and new models, and experiment.

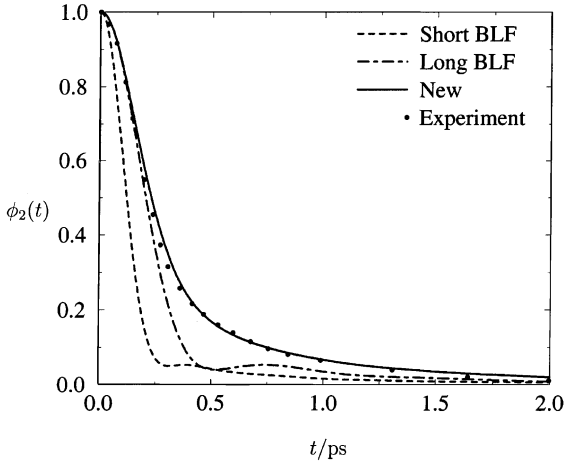

Fig. 3. Second-rank rotational time-correlation function for liquid oxygen at 77 K and 1 atm pressure: simulation results for the three models, and experiment.

3.2. Rotational dynamics

We next turn to the rotational dynamics of the liquid. Rotational dynamics are most easily characterized by the rank l time-correlation functions

$$\phi_l(t) = \left\langle P_l(\hat{u}(0) \cdot \hat{u}(t)) \right\rangle, \tag{4}$$

where $\hat{u}(t)$ is the unit vector parallel to the molecular bond, and $P_l(x)$ is the lth Legendre polynomial. For systems with a clear separation of time scales between rotational motion, vibrational dephasing, and vibrational energy relaxation, the depolarized Raman spectrum is proportional to the Fourier transform of the above time-correlation function with $l = 2$ [31]. This time-correlation function can then be obtained from experiment by inverse Fourier transformation.

The simulation results for $\phi_2(t)$ for the three (short BLF, long BLF, and new) models are shown in Fig. 3, together with the experimentally determined $\phi_2(t)$ from the depolarized Raman spectrum, from [23, Fig. 4]. The result for the new potential is in excellent agreement with experiment, while the results for the other two models are in poorer agreement. The two BLF models exhibit a small recurrence at intermediate times, showing that in these cases the molecules are undergoing freer rotation than in the new model, as a result of the shorter site–site distance. The time scale for this recurrence is shorter for the short BLF model than the long BLF model, due to the shorter bond length (and thus smaller moment of inertia) of the former.

3.3. Diffusion constant

Our results for the self-diffusion constant are listed in Table 2 for the three models. The diffusion constant was calculated both from the slope of the mean-squared displacement at long times and from the integral of the velocity time-correlation function [32], and the results of these two procedures agreed very well (<1%) for each of the three models. As can be seen, the diffusion constant is moderately sensitive to the potential, and quite insensitive to the moment of inertia (cf. the two BLF models). Unfortunately, we have been unable to find the experimental self-diffusion constant for liquid oxygen in the literature, and so have nothing to compare to here.

4. Summary and conclusion

We have determined a new model potential for liquid oxygen. Similar to the BLF potential [4], the new model adequately reproduces the thermody-

namics in the liquid state. However, in contrast to two different versions of the BLF model, the new model produces results that are in excellent agreement with experiment for the static structure factor (or the radial distribution function), and the second-rank time-correlation function for rotational dynamics. Armed with this potential, in future works [33,34] we will describe our calculations of the shift and width of the isotropic Raman spectrum for liquid oxygen, and will revisit the problem of vibrational energy relaxation in liquid oxygen [2]. (Of course for these problems we need to consider explicitly intramolecular vibrations; nonetheless, the non-vibrating model discussed herein is the foundation for these calculations.) In both cases we find that the new potential leads to good agreement of theoretical results with experiment [1,35].

Acknowledgements

The authors are grateful for support from the National Science Foundation (Grant Nos. CHE-9520619, CHE-9981539, CHE-9816235 and CHE-9522057). K.F.E. thanks Rakwoo Chang for assistance with the calculation of the static structure factor.

References

[1] B. Faltermeier, R. Protz, M. Maier, Chem. Phys. 62 (1981) 377.
[2] K.F. Everitt, S.A. Egorov, J.L. Skinner, Chem. Phys. 235 (1998) 115.
[3] S.A. Egorov, K.F. Everitt, J.L. Skinner, J. Phys. Chem. A 103 (1999) 9494.
[4] M. Bohn, R. Lustig, J. Fischer, Fluid Phase Equil. 25 (1986) 251.
[5] J.R. Sweet, W.A. Steele, J. Chem. Phys. 47 (1967) 3029.
[6] J.C. Laufer, G.E. Leroi, J. Chem. Phys. 55 (1971) 993.
[7] W.A. Steele, G. Birnbaum, J. Chem. Phys. 72 (1980) 2250.
[8] S. Nosé, M.L. Klein, Can. J. Phys. 60 (1982) 1365.
[9] T.W. Zerda, X. Song, J. Jonas, B.M. Ladanyi, L.C. Geiger, J. Chem. Phys. 87 (1987) 840.
[10] Y. Miyano, Fluid Phase Equil. 104 (1995) 71.
[11] B. Saager, J. Fischer, Fluid Phase Equil. 66 (1991) 103.
[12] C. Kriebel, A. Müller, J. Winkelmann, J. Fischer, Mol. Phys. 84 (1995) 381.
[13] A. Chahid, F.J. Bermejo, E. Enciso, M. García-Hernández, J.L. Martínez, J. Phys. Cond. Matt. 5 (1993) 423.
[14] D. Frenkel, J.P. McTague, J. Chem. Phys. 72 (1980) 2801.
[15] B.M. Ladanyi, J. Chem. Phys. 78 (1983) 2189.
[16] B.M. Ladanyi, L.C. Geiger, T.W. Zerda, X. Song, J. Jonas, J. Chem. Phys. 89 (1988) 660.
[17] A. Barreau, A. Chave, B. Dumon, M. Thibeau, B.M. Ladanyi, Mol. Phys. 67 (1989) 1241.
[18] P.S.Y. Cheung, J.G. Powles, Mol. Phys. 30 (1975) 921.
[19] R. Schmidt, W. Wagner, Fluid Phase Equil. 19 (1985) 175.
[20] H.W. Furomoto, C.H. Shaw, Phys. Fluids 7 (1964) 1026.
[21] P.W. Schmidt, C.W. Tompson, in: H.L. Frisch, Z.W. Salsburg (Eds.), Simple Dense Fluids, Academic Press, New York, 1968.
[22] J.C. Dore, G. Walford, D.I. Page, Mol. Phys. 29 (1975) 565.
[23] J. Bruining, J.H.R. Clarke, Mol. Phys. 31 (1976) 1425.
[24] L. Verlet, Phys. Rev. 159 (1967) 98.
[25] K. Singer, A. Taylor, J.V.L. Singer, Mol. Phys. 33 (1977) 1757.
[26] M.P. Allen, D.J. Tildesley, Computer Simulation of Liquids, Clarendon Press, Oxford, 1987.
[27] J.-P. Hansen, I.R. McDonald, Theory of Simple Liquids, 2nd ed., Academic Press, London, 1986.
[28] C. Andreani, J.C. Dore, F.P. Ricci, Rep. Prog. Phys. 54 (1991) 731.
[29] W.H. Press, B.P. Flannery, S.A. Teukolsky, W.T. Vetterling, Numerical Recipes, Cambridge University Press, Cambridge, 1986.
[30] R.J.L. de Carvalho, R. Evans, D.C. Hoyle, J.R. Henderson, J. Phys. Cond. Matt. 6 (1994) 9275.
[31] R.G. Gordon, Adv. Mag. Res. 3 (1968) 1.
[32] D.A. McQuarrie, Statistical Mechanics, Harper and Row, New York, 1976.
[33] K.F. Everitt, J.L. Skinner, J. Chem. Phys., in press.
[34] K.F. Everitt, J.L. Skinner, B.M. Ladanyi, J. Chem. Phys., in press.
[35] M.J. Clouter, H. Kiefte, R.K. Jain, J. Chem. Phys. 73 (1980) 673.